Journal of Advanced Research (2010) 1, 315–322

Cairo University

Journal of Advanced Research

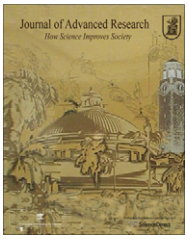

ORIGINAL ARTICLE

Lake Nasser evaporation reduction study

Hala M.I. Ebaid [a,*], **Sherine S. Ismail** [b]

[a] *Survey Research Institute, Delta Barrage, Cairo 13621, Egypt*
[b] *Nile Research Institute, Delta Barrage, Cairo 13621, Egypt*

Received 4 March 2010; revised 13 May 2010; accepted 8 June 2010
Available online 20 October 2010

KEYWORDS

Remote sensing;
Landsat;
GIS;
Evaporation;
Lake Nasser

Abstract This study aims to evaluate the reduction of evaporation of Lake Nasser's water caused by disconnecting (fully or partially) some of its secondary channels (khors). This evaluation integrates remote sensing, Geographic Information System (GIS) techniques, aerodynamic principles, and Landsat7 ETM+ images. Three main procedures were carried out in this study; the first derived the surface temperature from Landsat thermal band; the second derived evaporation depth and approximate evaporation volume for the entire lake, and quantified evaporation loss to the secondary channels' level over one month (March) by applied aerodynamic principles on surface temperature of the raster data; the third procedure applied GIS suitability analysis to determine which of these secondary channels (khors) should be disconnected. The results showed evaporation depth ranging from 2.73 mm/day at the middle of the lake to 9.58 mm/day at the edge. The evaporated water-loss value throughout the entire lake was about 0.86 billion m^3/month (March). The analysis suggests that it is possible to save an approximate total evaporation volume loss of 19.7 million m^3/month (March), and thus 2.4 billion m^3/year, by disconnecting two khors with approximate construction heights of 8 m and 15 m. In conclusion, remote sensing and GIS are useful for applications in remote locations where field-based information is not readily available and thus recommended for decision makers remotely planning in water conservation and management.

Introduction

Lake Nasser is one of the largest man-made fresh-water reservoirs in the world. It was formed due to the construction of the Aswan High Dam during the 1960s. It is an elongated body of water about 500 km long, upstream from the Aswan High Dam, about 170 km of which is in Sudan, where it is called Lake Nubia. The average width of the lake is about 12 km. The water volume in the lake fluctuates annually and seasonally, depending on the net annual volume of water it receives and the operation of the High Dam [1].

The highest recorded water level was 181.6 m in November 1999, while the lowest level recorded so far was 158 m in July 1988 (above mean sea level) [2]. The lake covers a total surface

* Corresponding author. Tel.: +20 106933474; fax: +20 242187152.
E-mail address: hala_sri@yahoo.com (H.M.I. Ebaid).

Peer review under responsibility of Cairo University.
doi:10.1016/j.jare.2010.09.002

Production and hosting by Elsevier

area of about 6000 km^2, 85% of which is in Egypt, and has a storage capacity of some 162 km^3 of water. The average depth is about 25 m and the maximum depth is 130 m [1].

Water loss from the lake is a national problem. The evaporated water loss ranges between 10 and 16 billion m^3 every year, which is equivalent to 20–30% of the Egyptian income from Nile water [3].

Remote Sensing (RS) and Geographical Information System (GIS) data play a rapidly increasing role in the field of hydrology and water resources development.

Theories and formulas abound to obtain accurate estimates of lake evaporation. Common examples pertaining to evaporation are the Penman, the Hargreave, and the Hamon equations. Although these methods are simple, they yield accurate results [4]. Subsequent to these, Shaltout [3] used the Meteosat infra-red window (10.5–12.5 μm) observations and empirical models. He estimated the evaporated water every day and determined the yearly water loss from the integration of daily values. In addition, the Bulk-Aerodynamic Method utilizes the skin temperature of water, relative humidity, wind speed, and air temperature to estimate evaporation, from Advanced Spaceborne Thermal Emission and Reflection Radiometer (ASTER) images of Elephant Reservoir in New Mexico [5]. This method shows a difference in temperature of 1.7 °C and in evaporation rate of 1.2426 mm/day, between Aster images and when measured; these are considered good results. The most commonly used method to calculate evaporation of the Great Lakes utilizes air, surface water temperature, wind speed, and humidity data [6].

The main objectives of the present study include:

(1) Calculating evaporation rate per day and monthly water loss from the integration of daily values. This is done with a chain group of raster calculator tools that apply the Bulk-Aerodynamic principle over surface temperature images obtained from Landsat 7 ETM+ Satellite images (March 2002).
(2) Analyzing and evaluating scenarios that show the impact of disconnecting some of the secondary channels from Lake Nasser using the GIS suitability analysis tool, and taking into consideration economic and environmental factors. In this way, the project has the advantage of satellite thermal data and GIS spatial tools for better planning and allocation of water resources.

Methodology

Site description

Lake Nasser extends from southern Egypt to the northeast part of Sudan. This research is limited to the Egyptian portion that extends along the eastern desert. Lake Nasser's length is about 500 km; its maximum width is 35 km. The total area surveyed is approximately 50,000 feddans. In general, the geographic boundary is between latitude 21° and 24° 30 north and longitude 31° 30 and 33° east.

Preprocessing images

1. *Satellite data used:* Remotely sensed data (4 Landsat ETM+ images) were adopted in this research. The image data from March 2002 were acquired from the Internet in GeoTIFF format [7] (image data were selected for this specific month and year due to availability of the complete set). Table 1 illustrates the characteristics of these images.
2. *Georeferencing images:* Acquired Landsat images were mosaicked, then corrected geometrically with ERDASS IMAGINE using a pre-georeferenced, mosaicked topographic map (with projection: Universal Transverse Mercator (UTM), World Geodetic System 1984 (WGS84), Zone 36 N), which covers the same part of the lake. The map is from the Egyptian Survey Authority 1991 (Fig. 1).
3. The georeferenced image was then categorized with an unsupervised classification tool to obtain the water body class of Lake Nasser, because classification of Landsat images is considered the best technique for water texture recognition (Fig. 2).
4. Accurate measurement of Lake Nasser's area was derived in vector format by applying ArcGIS Raster to the vector tool.

Deriving lake surface temperature from the Landsat thermal band

– Conversion of the Digital Number (DN) to spectral radiance ($L\lambda$). The spectral radiance ($L\lambda$) is calculated by applying the following equation using the Raster calculator tool [8]:

$$L\lambda = ((\mathrm{LMAX} - \mathrm{LMIN})/(\mathrm{QCALMAX} - \mathrm{QCALMIN})) * (\mathrm{QCAL} - \mathrm{QCALMIN}) + \mathrm{LMIN} \quad (1)$$

where

– QCALMIN = 1, QCALMAX = 255 and QCAL = Digital Number.
– The LMINs and LMAXs are the spectral radiances for band 6 at digital numbers 1 and 255, respectively.
– Conversion of the spectral radiance to temperature.

The ETM+ thermal band data can be converted from the spectral radiance black body to temperature, which assumes surface emissivity = 1 [8]:

$$T = K2/\ln(K1/L\lambda + 1) \quad (2)$$

where

– T = Effective at satellite temperature in Kelvin,
– $K1$ = Calibration constant 1 (watts/meter squared∗–ster∗μm) (666.09),
– $K2$ = Calibration constant 2 (Kelvin) (1282.71),
– $L\lambda$ = Spectral radiance (watts/meter squared∗ster∗μm).

The above equations were applied on the Land sat thermal band 6 using a map algebra tool under the ArcGIS environment to derive surface temperature in °C.

Deriving approximate evaporation depth and evaporation volume by applying the aerodynamic principle on the derived surface temperature raster data

In this procedure, the aerodynamic equation was applied on surface temperature raster data to evaluate evaporation rate.

Table 1 Acquiring data.

Acquisition date	Path/row	Band combination	Scene_time	Pixel size	Cloud%	Sun elevation angle
Mar 15, 2002	175/044	12345678	08:08:32	PAN = 15 THM = 60	0	52.4725
Mar 15, 2002	175/045	12345678	08:08:55		0	53.1720
Mar 8, 2002	174/044	12345678	08:02:25		0	50.2034
Mar 8, 2002	174/043	12345678	08:08:16		0	63.8762

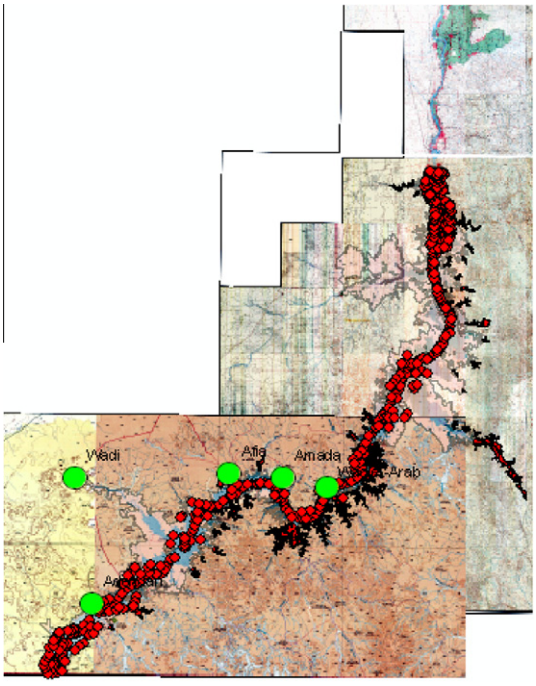

Fig. 1 Mosaiced topographic map overlaid by DEM points layer.

Aerodynamic equations:

$$\text{Evaporation rate [mm day}^{-1}] = K_E U(e_s - e_a)(86.4 \times 10^6) \quad (3)$$

$$e = e_s(R_H)/(100) \quad (4)$$

where K_E is determined as follows:

$$K_E = \frac{0.622\rho_a \times (0.4)^2}{P\rho_w\left[\ln\left\langle\frac{z_m - z_d}{z_0}\right\rangle\right]}2 \quad (5)$$

The air's saturation vapour pressure, es, is a property dependent on temperature and estimated by polynomial function [9]. Water surface temperature or "skin" temperature was used to determine the saturation vapour pressure at the water's surface. Vapour pressure of the air was determined by multiplying relative humidity by saturated vapour pressure. In this case, the saturated vapour pressure of air was determined by using the air temperature.

$$e = \frac{a_0 + T(a_1 + T(a_2 + T(a_3 + T(a_4 + T(a_5 + a_6 T)))))}{10} \quad (6)$$

Eq. (6) was applied on the surface temperature raster data deduced from the previous procedure to produce e_s raster data, and this was again applied to the average air temperature for Lake Nasser by multiplying with relative humidity to get e_a using the raster tool.

Monthly evaporation volume (for March) was calculated by multiplying deduced (E) by factor .03∗area (in m^2) to transform evaporation rate in mm/day to evaporation volume in m^3/month. This value was quantified to secondary channel levels using ArcGIS tools.

Applying GIS suitability analysis to select secondary channels (khors) to be disconnected to reduce evaporation volume

To perform this suitability analysis, the following steps were undertaken:

1. Applied GIS techniques to select and extract data for 75 secondary channels (khors) from Lake Nasser for analysis (Fig. 3).
2. Defined the analysis criteria:
   - Maximum evaporation volumes from secondary channels for maximum evaporation reduction.
   - Minimum average water depth values for all secondary channels for economic consideration.
   - Minimum width length (at positions where the khors will be disconnected) for all secondary channels for effort and cost savings.
3. Listed and collected data needed for this analysis, which comprises the following:
   - Digital Elevation Model (The source of these data is the Nile Research Institute database, with accuracy about sub meter [2]) of Lake Nasser, to calculate water depth for all secondary channels.
   - Width at positions where the khors will be disconnected for all secondary channels of the lake.
   - Evaporation volume data for the study period (March 2002) for all water secondary channels.
4. Intersected the 3 main processed layers that produced a vector layer with 13 secondary channels (khors), where they best fit the previously mentioned criteria using Select-by attributes.

General assumptions

There are some assumptions that go into research calculations for simplicity, and are described as follows:

- The wind speed is assumed to be constant (the average value of 3 hydro climatic stations from Table 2) throughout the entire lake.
- Air temperature and percentage of relative humidity were based on the monthly mean daily values. There was a maximum difference of 3 °C between average daily temperatures on a specific day (March 8 and 15) and monthly mean daily values of air temperature (March) for all meteorological sta-

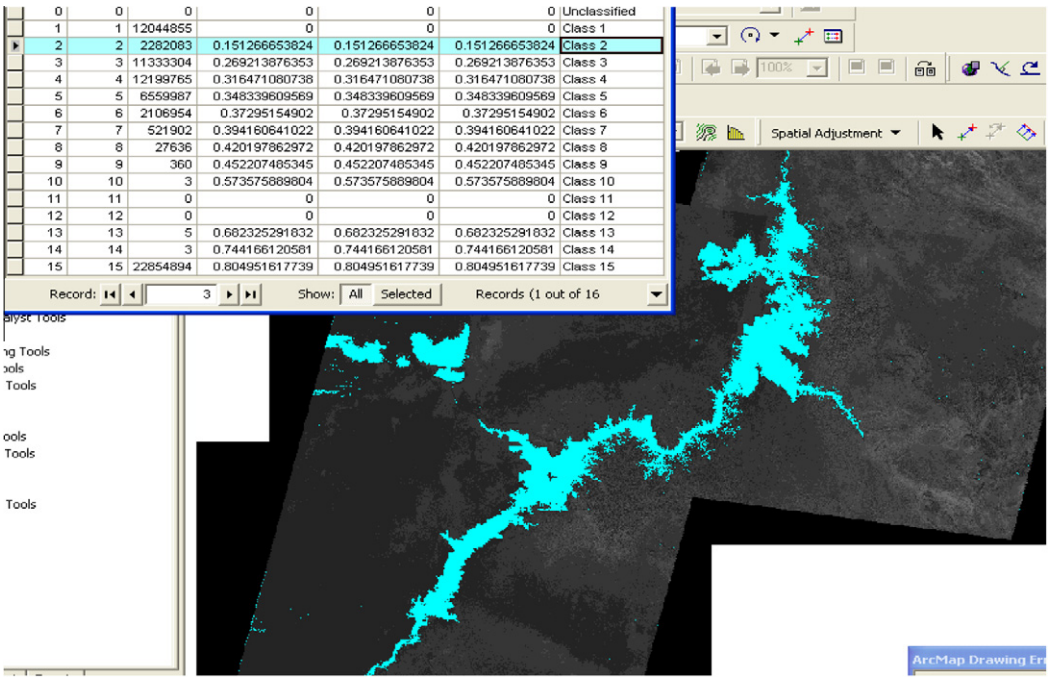

Fig. 2 Water class represents Lake Nasser and Toshka depression.

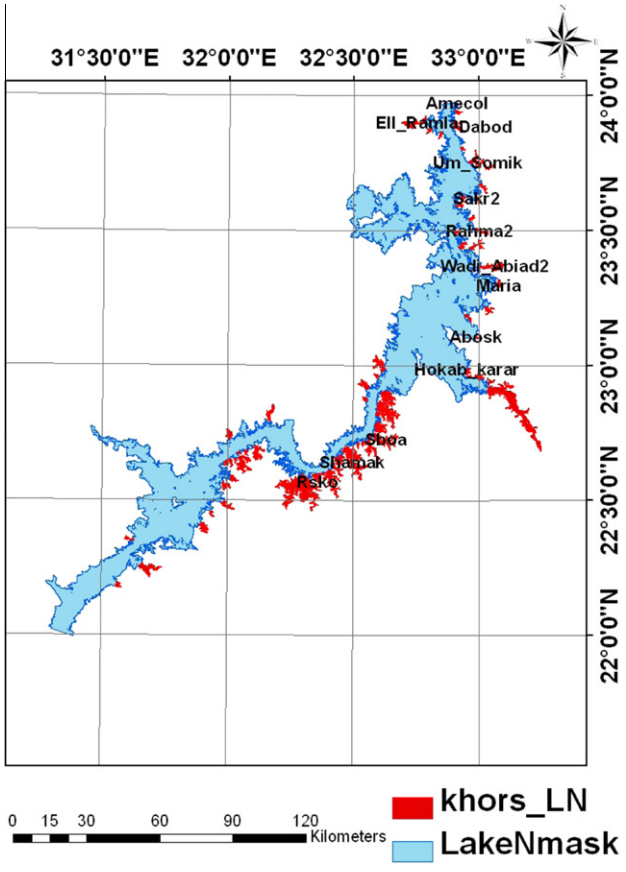

Fig. 3 Lake Nasser (2002) with 75 derived secondary water channels (khors).

tions around the lake, and also there is a correlation between the average monthly air temperature and average daily temperature for all these stations ($r = 0.873$). The monthly average values for air temperature and relative humidity were used in the Bulk-Aerodynamic equation for an approximate calculation of evaporation values; however, the variation of air temperature and relative humidity were considered for all days of the month (Fig. 4).

– Another approximation is the calculation of evaporation loss per month, which depends only on the two image dates acquired at (March 8 and 15, 2002), and luckily the images are from mid-March, and thus can reasonably be assumed to represent average climatic parameters values.

Results and discussion

1. From the Water Surface Temperature (WST) map in °C, which was deduced from the Landsat-7 ETM thermal band, it is clear which khor locations represent the lake's boundary gain maximum WST values (Fig. 5).
2. The raster evaporation depth map in mm/day was obtained by applying the Bulk-Aerodynamic formulas on the surface

Table 2 Wind speed values.

Station's location	Wind speed at 2 m above the lake's surface, monthly mean daily values (March 2002) (m/s)
2 km in front of the High Dam	3
75 km in front of the High Dam	2.2
280 km in front of the High Dam	4
Average wind speed = 3.06 m/s	

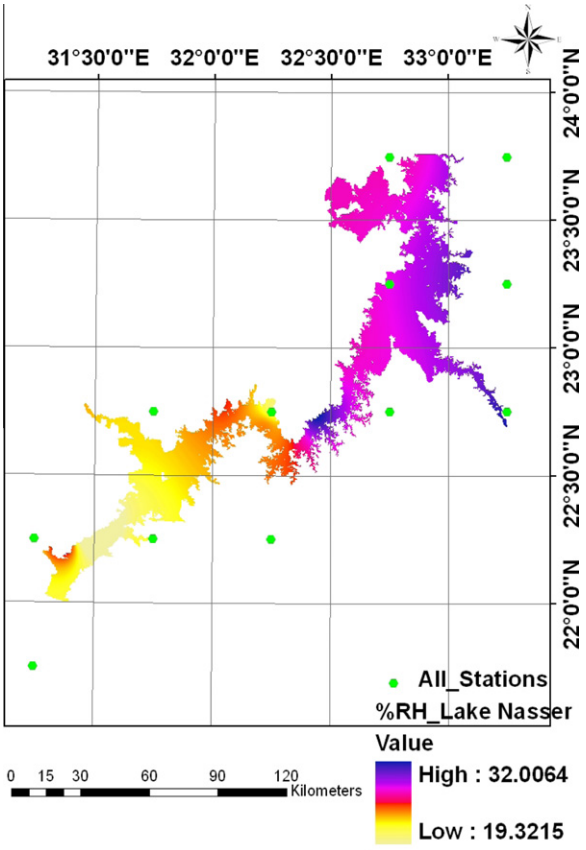

Fig. 4 Station's air temperature and RH values.

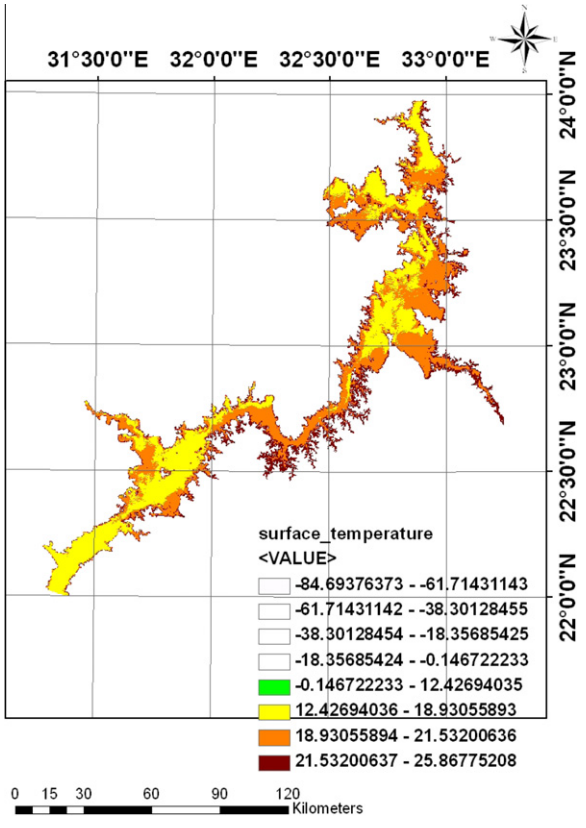

Fig. 5 Surface temperature distribution over the entire lake.

temperature raster image, which were applied to the monthly average atmospheric parameters values from meteorological stations around the entire lake (wind speed, air temperature, and atmospheric pressure), and also to the temporal Climate Dataset (March 2002) from the Climatic Research Unit [10].

Evaporation depth in mm/day reached maximum values near secondary channels due to proximity to land where the temperature is higher. Fig. 6 shows evaporation depth values, which ranged approximately from 5 to 10 at secondary channels locations, and from 2 to 5 at the middle of the lake.

3. From the previous analysis, it was clear that there is a strong correlation ($R^2 = 0.98$, coefficient of determination) between surface temperature in °C and evaporation depth in mm/day.
4. Also, it is possible to reduce evaporation loss and consequently save some of the lake's water by disconnecting some of the secondary channels (khors) where the evaporation losses are higher.
5. Average water depth values were derived with lake's water level at 179.15 m (March 2002). Average water depths were calculated for every water secondary channels (Fig. 7), and characteristic data for all secondary water channels were stored in the ArcGIS geodatabase.
6. ArcGIS suitability analysis was applied to select the most suitable secondary water channels (khors) to be disconnected.

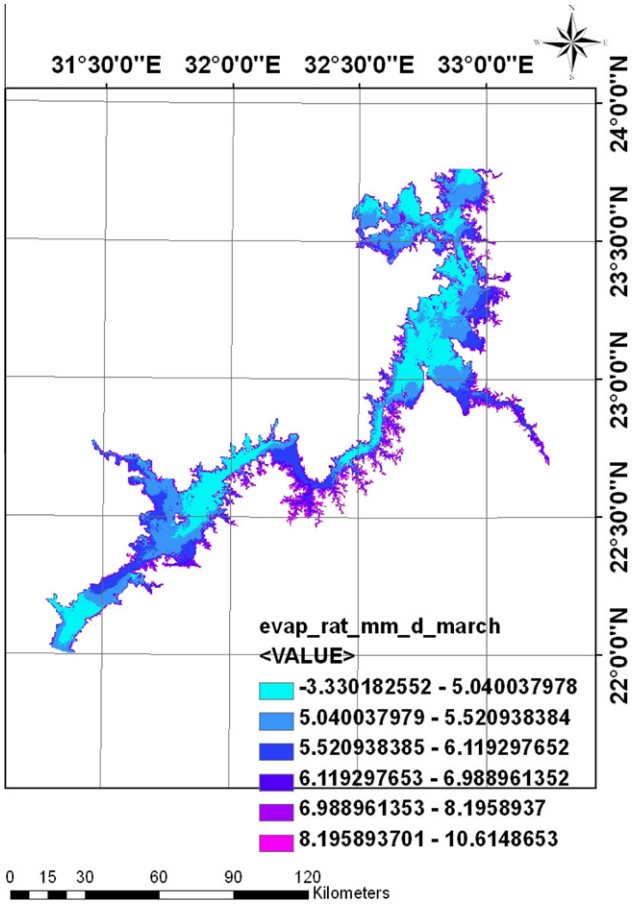

Fig. 6 The distribution of evaporation depth in mm/day throughout the entire lake.

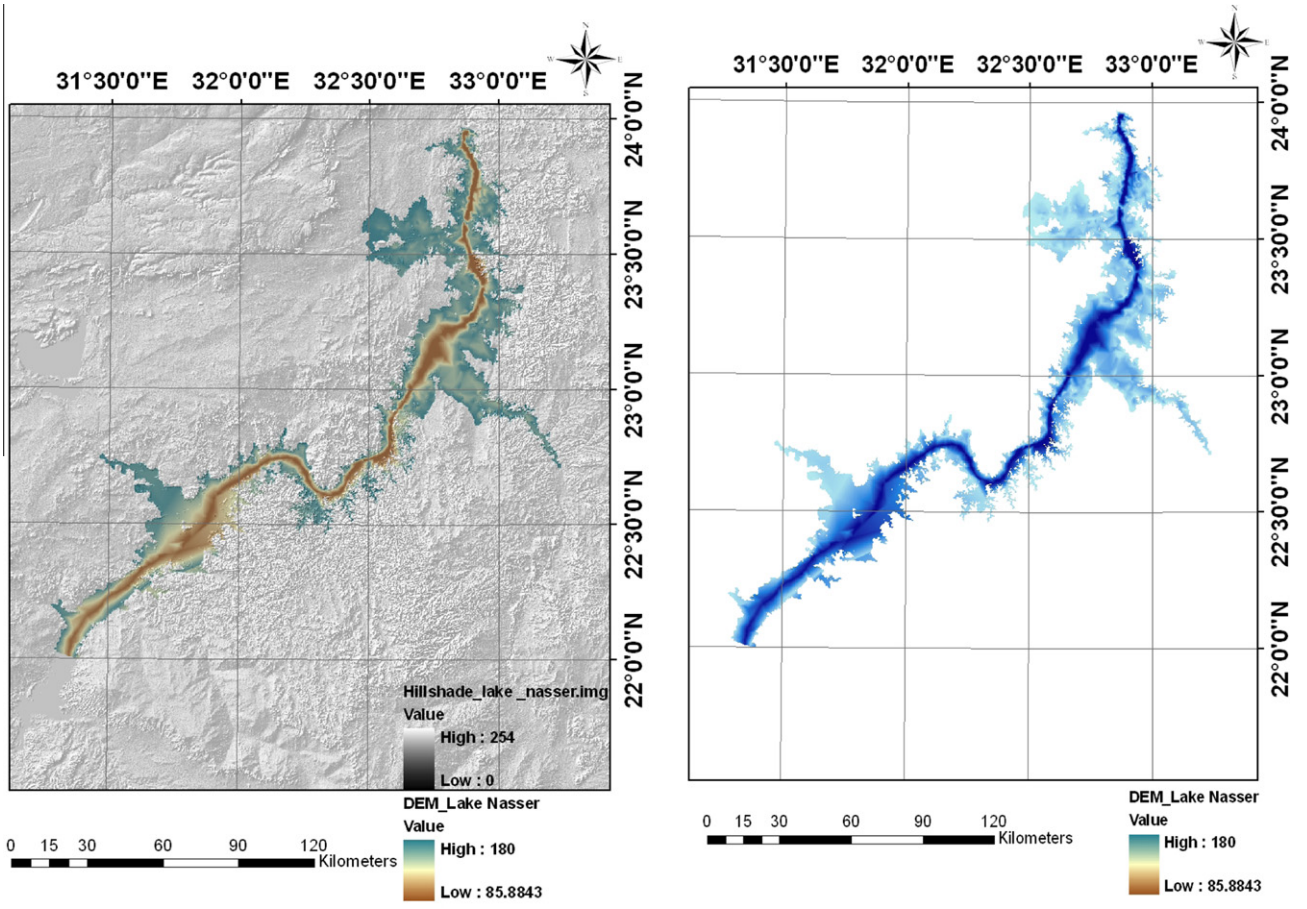

Fig. 7 Lake's DEM and average water depth.

The results in Table 3 demonstrate the characteristics of 13 secondary water channels, as an output layer from the GIS suitability analysis.

7. The authors thus recommend 13 secondary channels as most reasonable to disconnect from Lake Nasser in order to reduce the water evaporation rate. There are two options; the first is to disconnect five khors in different places with relatively lower Dam length and reasonable conservation potential. The second option is to disconnect the two khors with the most significant potential for evaporation reduction. Decision makers may choose between these; however, the authors recommended the second option.

The first choice

Disconnect five secondary channels, as indicated in Table 4. Consequently, five dams should be designed with dams-length values ranging from 240 m to 543 m, with an approximate summed up dam-length values of 2133 m, and an approximate maximum dam height of 16 m. This will result in an approximate total evaporation volume loss of 12 million m^3/month.

The second alternative

Disconnect two secondary channels, as indicated in Table 5. Consequently, 2 dams should be designed with approximate dimensions: total dam length = 1781 m, and dam height > average water depth values (8.11 m and 15.17 m), to save an approximate total evaporation volume loss of 19.7 million m^3/month.

8. This work estimates the evaporation loss specifically for March 2002 (due to availability of data). This month has seasonally lower evaporation rates, and consequently, the evaporation volume losses in August with increased air temperature will be higher and thus water can be conserved with the disconnection of these selected khors.
9. Finally, another important aspect must be considered for dam design, which is environmental preservation. This can be incorporated by designing the proposed dam with gates (partially disconnected) to allow a minimum water depth flow to the secondary water channels to attract the same birds, fish, and animals that live in these areas.
10. The detailed design of the dam and the cost of dam construction were considered out of scope for this study. However, it is bound to be advantageous to build the dams regardless of cost due to the following reasons: first, the dam may be constructed with local lake-deposited material; this will reduce the lake's storage capacity as well as build a dam to reduce evaporation. Second, dam construction is a singular cost, but the water savings would be long term. Third, the water conserved is priceless with the increasing water scarcity in the region and in the whole world.

Table 3 Suitability analysis results.

No.	khor_name	khor_area (m^2)	Code	Dam length (m)	Evapo (m^3/month)	khor_average_water depth (m)
1		87,44,400	48	468.62	19,04,405	7.67
2	Shamak	250,11,000	40	1360.29	54,57,562	10.62
3		208,94,400	31	543.32	45,50,438	15.17
4		61,20,000	68	976.73	11,65,375	10.56
5	Wadi_Alaqi	712,33,200	29	1236.93	151,41,062	8.11
6	Wadi_Abiad2	111,07,800	15	516.14	24,01,294	4.73
7	Rahma2	45,50,400	10	240.00	991,193	5.53
8	Um_Somik	95,86,800	4	364.97	20,90,822	9.22
9		86,27,400	73	917.82	16,64,828	4.93
10		108,32,400	70	969.33	21,77,637	12.38
11		66,40,200	66	662.72	11,80,970	3.48
12		60,82,200	65	763.68	10,21,969	3.94
13		124,23,600	43	1482.10	28,87,919	11.12

Table 4 Water secondary channels (first choice).

No.	khors_name	khors_area (m^2)	Code	Dam_length (m)	Evaporation (million m^3/month)	Water depth (m)
1		208,94,400	31	543.32	4.550438	15.17
2	Wadi_alaqi	712,33,200	29	1236.93	15.141062	8.11

Table 5 Water secondary channels (second choice).

No.	khors name	khors_area (m^2)	Code	Dam_length (m)	Evaporation (million m^3/month)	Water depth (m)
1		8744400.0	48	468.615	1.9	7.672
2		20894400.0	31	543.323	4.6	15.167
3	Wadi_Abiad2	11107800.0	15	516.140	2.4	4.732
4	Rahma2	4550400.0	10	240.000	.99	5.527
5	Um_Somik	9586800.0	4	364.966	2.1	9.217

Conclusions

Using remote sensing and GIS analysis is effective and is recommended for selecting the most reasonable secondary channels (khors) to disconnect from Lake Nasser in order to reduce the water evaporation rate. The analysis demonstrated that in a month like March, it is possible to save an approximate total evaporation volume loss of 19.7 million m^3. This translates to 2.4 billion m^3/year as a result of closing two khors with constructions heights of about 8 m and 15 m. With this information, decision makers can remotely plan needed actions in water savings and management.

Recommendations

This study would benefit from an analysis of more images from different dates. More research is needed to continue this inquiry and to form a database for lake evaporation metrics and the potential impacts of disconnecting various khors.

Acknowledgment

The authors gratefully acknowledge the assistance of Dr. Medhat Aziz, the director of the Nile Research Institute, for his helpful comments on the manuscript.

Appendix

E	evaporation rate [mm day^{-1}]
K_E	coefficient [kPa^{-1}]
u	wind speed measured at 2 m above the surface as standard [m s^{-1}]
e_s	saturation vapour pressure at the water surface [kPa]
e_a	vapour pressure of the air above the water surface [kPa]
K_E	coefficient of efficiency of vertical transport of water vapour by eddies of the wind [kPa^{-1}]
ρ_a	density of air [1.220 kg m^{-3}]
ρ_w	density of water [1000 kg m^{-3}]
P	atmospheric pressure [kPa]
Z_m	height at which wind speed and air vapour pressure are measured [m]
Z_d	zero-place displacement [m]; $Z_d = 0$ over typical water surfaces
Z_o	roughness height of the surface [m]; $Z_0 = 2.30 \times 10^{-4}$ m over typical water surfaces
es	saturation vapour pressure [kPa]
T	temperature [°C]
λ	wavelength of emitted radiance
α	hc/K (1.438×10^{-2} mK)
h	Planck's constant (6.26×10^{-34} J s)
c	velocity of light (2.998×10^{8} m/s)
K	Stefan Bolzmann's constant (1.38×10^{-23} J/K)
$a_{1\ to\ 6}$	constant values

References

[1] Elewa HH. Water resources and geomorphological characteristics of Tushka and west of Lake Nasser. Egypt Hydrogeol J 2006;14(6):942–54.
[2] Nile Research Institute. Nile Research Institute Database. Egypt: Nile Research Institute, National Water Research Center; 2010.
[3] Mosalam Shaltout MA, El Housry T. Estimating the evaporation over Nasser Lake in the Upper Egypt from Meteosat observations. Adv Space Res 1997;19(3):515–8.
[4] Salas JD. Notes on evaporation and evapotranspiration. CE Report 322. Colorado State University: Department of Civil and Environmental Engineering; 2004.
[5] Herting A, Tim F, Jordan E. Mapping of the evaporative loss from Elephant Butte Reservoir using remote sensing and GIS technology. Mexico: New Mexico State University (NMSU); 2004.
[6] Croley TE, Hunter TS, Martin SK. Great lakes monthly hydrologic data. NOAA Technical Report, USA; 2001.
[7] USGS Organization Internet Site, USA. http://earthexplorer.usgs.gov; 2010.
[8] Homer C, Cheng H, Limin Y, Bruce W, Michael C. Landsat 7 science data user's handbook. USA: Raytheon ITSS, USGS/EROS Data Center; 2001.
[9] Lowe PR. An approximating polynomial for the computation of saturation vapor pressure. J Appl Meteorol 2004;16(4):100–3.
[10] CGIAR International Research Centers internet site, Columbia. http://cru.csi.cgiar.org; 2009.